Accepted Manuscript

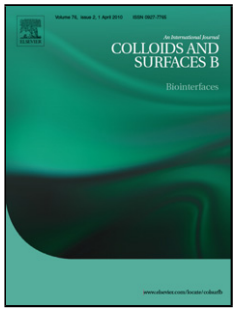

Title: The Effects of Biomimetically Conjugated VEGF on Osteogenesis and Angiogenesis of MSCs (Human and Rat) and HUVECs Co-culture Models

Authors: Lanxin L*ü*, Anthony Deegan, Faiza Musa, Tie Xu, Ying Yang

PII: S0927-7765(18)30273-X
DOI: https://doi.org/10.1016/j.colsurfb.2018.04.060
Reference: COLSUB 9313

To appear in: *Colloids and Surfaces B: Biointerfaces*

Received date: 23-1-2018
Revised date: 9-4-2018
Accepted date: 29-4-2018

Please cite this article as: Lanxin L*ü*, Anthony Deegan, Faiza Musa, Tie Xu, Ying Yang, The Effects of Biomimetically Conjugated VEGF on Osteogenesis and Angiogenesis of MSCs (Human and Rat) and HUVECs Co-culture Models, Colloids and Surfaces B: Biointerfaces https://doi.org/10.1016/j.colsurfb.2018.04.060

The Effects of Biomimetically Conjugated VEGF on Osteogenesis and Angiogenesis of MSCs (Human and Rat) and HUVECs Co-culture Models

Lanxin Lü [1, 2], Anthony Deegan [2], Faiza Musa [2], Tie Xu [1]*, Ying Yang [2]*

[1] Emergency Center of the Affiliated Hospital of Xuzhou Medical University; Institute of Emergency Rescue Medicine, Xuzhou Medical University, Xuzhou, 221002, China

[2] Institute for Science and Technology in Medicine, School of Medicine, Keele University, Stoke-on-Trent, ST4 7QB, UK

***Corresponding authors**

Professor Tie Xu

Email: xutie889@163.com

Professor Ying Yang

Email: y.yang@keele.ac.uk

Graphical abstract

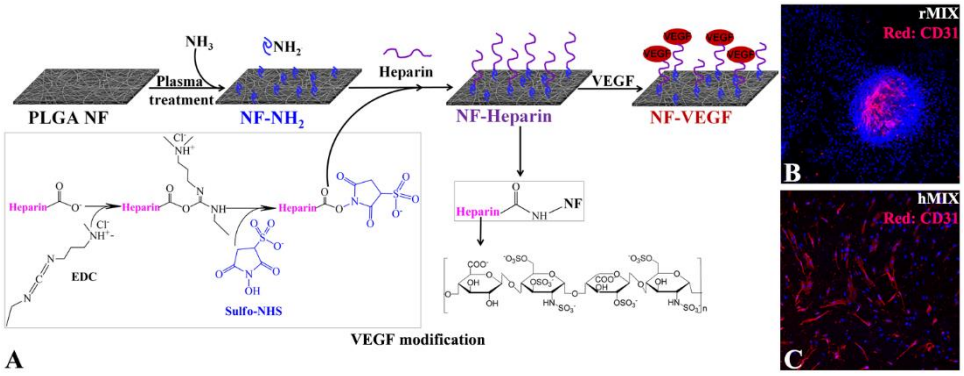

Highlights

- VEGF was biomimetically conjugated onto PLGA NF scaffolds through heparin
- The grafting technique fulfilled the sustained release and bioactivity of VEGF
- Conjugated VEGF and co-culture with HUVECs regulated MSCs' activities
- Osteogenesis and angiogenesis differentiation of MSCs were specie dependent

Abstract

The purpose of this work was to investigate if the biomimetically conjugated VEGF and HUVECs co-culture could modulate the osteogenic and angiogenic differentiation of MSCs derived from rat and human bone marrow (rMSCs and hMSCs). After treated by ammonia plasma, Poly(lactic-co-glycolic acid) (PLGA) electrospun nanofibers were immobilized with VEGF through heparin to fulfil the sustained release. The proliferation capacity of rMSCs and hMSCs on neat PLGA nanofibers (NF) and VEGF immobilized NF (NF-VEGF) surfaces were assessed by CCK-8 and compared when MSCs were mono-cultured and co-cultured with HUVECs. The effect of VEGF and HUVECs co-culturing on osteogenic and angiogenic

differentiation of rMSCs and hMSCs were investigated by calcium deposits and CD31 expression on NF and NF-VEGF surfaces. The results indicated that VEGF has been biomimetically immobilized onto PLGA nanofibers surface and kept sustained release successfully. The CD31 staining results showed that both VEGF and HUVEC co-culture could enhance the angiogenesis of rMSCs and hMSCs. However, the proliferation and osteogenic differentiation of MSCs when cultured with VEGF and HUVECs showed a species dependent response. Taken together, VEGF immobilization and co-culture with HUVECs promoted angiogenesis of MSCs, indicating a good strategy for vascularization in bone tissue engineering.

Keywords: MSCs, HUVECs, co-culture, osteogenic, angiogenic

Introduction

The main challenge for bone tissue engineering is to integrate the generated new bones with host to perform their function [1]. Many scaffolds have been developed and employed to induce bone formation for long bone defect repair. One limitation of these studies is the low diffusion of oxygen and nutrition in the engineered products due to lack of blood vessel networks [2, 3]. Current tissue engineering strategies for vascularization of bone scaffolds are

growth factors delivering and endothelial cells introducing to fabricate vascularized tissue engineering bone [4].

Vascular endothelial growth factor (VEGF), originally known as vascular permeability factor (VPF), is one of the most important proangiogenic factors that can stimulate new blood vessels formation during embryonic development and new vessels regeneration after injury [5, 6]. Several signaling pathways were activated by the binding of VEGF with its receptors, leading to increased survival, proliferation, penetration, and migration of cells [7], which can help blood vessel's rebuilding after injury. Therefore, VEGF is one of the most commonly used growth factor for vascularization in bone tissue engineering [8, 9]. While the half-life of VEGF is very short, only 6-8 hours. Stabilization of VEGF and achieving its sustained releasing are required for in vitro and in vivo application [4].

Encapsulation of growth factors by hydrogel and biodegradable polymers has been employed to realize their sustained releasing. Zhang et al had injected silk hydrogel encapsulated with VEGF and bone morphogenetic protein-2 (BMP-2) to the rabbit maxillary sinus floor to promote angiogenesis and new bone formation [10]. Degradable poly (DL-lactic acid) scaffolds encapsulated with VEGF and seeded with human bone marrow stromal cells exhibited increased bone volume and blood vessel formation following implantation in a mouse femur segmental defect [11]. Besides depending on the degradation of scaffolds, controlled delivery of growth factors can accomplished by covalent and affinity binding them

to scaffold's surface [4]. Polydopamine has been deposited onto the surface of poly(L-lactide-co-ε-caprolactone) to mediate the immobilization of VEGF for accelerating endothelialization of vascular grafts [12]. Previous studies have bonded a series of proteins through heparin, which can preserve the biological activity of proteins. Heparin, as part of proteoglycans, is ubiquitously present in the cell surface and extracellular matrices of mammalian cells. It has been demonstrated that heparin not only bind VEGF directly but also enhance VEGF binding to VEGF receptor 2 as a complex, ultimately controlling VEGF activity [13]. Heparin also provide an abundance of hydroxyl and carboxylic acid groups allowing it to be easily modified with reactive group of scaffolds [14, 15].

In addition to growth factor stimulation, another approach to achieve vascularization in bone tissue engineering is the recruitment of stem cells, endothelial cells and other cells to develop capillary and vessels. Mesenchymal stem cells (MSCs), derived from bone marrow, adipose tissue, umbilical cord et al, have low immunogenic property and multi-differentiation potential and were widely used in tissue engineering of bone, nerve, tendon and cartilage [16]. The immunosuppressive properties of MSCs, performing through modulating T-cell functions, may have therapeutic benefit for the transplantation of scaffolds with cells [16]. It has been demonstrated that MSCs co-cultured with human umbilical vein endothelial cells (HUVECs) achieved excellent osteogenic and angiogenic capability in vivo [17]. Ma et al. investigated the angiogenic capacity of MSCs co-culturing with HUVECs when implanted into mice and

evaluated the different healing effects of MSCs when derived from human bone marrow and adipose [18]. However there was no report whether the effect from MSCs when co-cultured with HUVECs is species dependent.

As an FDA-approved polymer, poly(D, L-lactic-co-glycolic acid) (PLGA) with adjustable degradation rate was used widely in tissue engineering to fabricate into scaffolds [19]. Electrospining PLGA into nanofibraous scaffolds has an advantage to biomimic native extracellular matrix. However, like most polyester polymers, PLGA is a hydrophobic polymer with no reactive group and recognition sites for cell attachment. Therefore, it is important to modify PLGA surface and introduce active biomolecules onto PLGA scaffolds to promote specific cell adhesion, proliferation and differentiation.

In this study, we developed a new technique to immobilize VEGF to synthetic nanofibrous scaffolds and evaluate its effects on osteogenic and angiogenic capacity of MSCs and HUVECs co-culture models. The MSCs from rat and human were used to study the species dependency. We hypothesize that biomimetically incorporation of VEGF can maximize its activities for sustained work period, and VEGF and co-culture conditions on osteogenisis and angiogenisis are cell species dependent.

Materials and Methods

Electrospun PLGA nanofibrous scaffolds

Poly(lactic-co-glycolic acid) (PLGA) nanofibrous scaffolds were fabricated by electrospun technique as described in our previous study [20]. Briefly, 3% PLGA (w/v) electrospinning solution was obtained by dissolving PLGA granule (200 K, Purac, Netherlands) in chloroform and N, N-dimethylformamide (3:1 v/v). The solution was delivered by a syringe at 1.5 mLh^{-1}. The distance between the syringe needle (positive electrode) and the collector (negative electrode) was 25 cm and the voltage was set as 15 kV. The formed PLGA nanofibrous (NF) scaffolds were stabilized on round coverslips and kept in vacuum oven overnight to evaporate the residue solvent and were sterile by immersing in 70% ethanol for 30 minutes. Scanning electron microscope (SEM, ultra plus Zeiss, Germany) was used to observe morphology of PLGA nanofibers.

Preparation of VEGF-modified PLGA electrospun scaffolds

VEGF was immobilized to PLGA NF by a two-step process as illustrated in Figure 1. The first process step was introduction of amine groups to the surface of PLGA through ammonia plasma treatment. In the second step of the process, heparin was grafted to the amine groups on the NF surface covalently, then VEGF was immobilized to the PLGA NF scaffolds through affinity binding.

Ammonia plasma treatment: Plasma treatment of PLGA NF scaffolds to graft amine groups was performed in a glow discharge stainless steel reactor (Diener electronic, Plasma-Surface-Technology, Germany). Scaffolds were put into the chamber and the reactor was evacuated to 21 mbar, followed by pumping ammonia gas and maintenance at 50 mbar. Plasma treatment was lasting for 5 minutes. The treated scaffolds were denoted as NF-NH_2.

Heparin crosslink through EDC/NHS: Heparin modification was accomplished by using 1-ethyl-3-(3-dimethylaminopropyl) carbodiimide hydrochloride (EDC) and N-hydroxysulfosuccinimide (Sulfo-NHS) as crosslink agents following an established protocol [21]. Briefly, EDC, sulfo-NHS, and heparin solution were added into 2-(morpholino) ethanesulfonic acid buffer with the final concentration of 2 mM, 5 mM, and 1 $mgmL^{-1}$ respectively and mixed for 15 minutes at room temperature to active the carboxylic group of heparin. β-mercaptoethanol was added with the final concentration of 20 mM to inactivate the EDC, after which increased the system pH to 7.0 by adding concentrated PBS. 500 μL of the mixed solution was added to NF-NH_2 scaffolds with the surface area of 0.8 cm^2 for 2 hour reacting at room temperature. Any remaining heparin was removed by washing the scaffolds with PBS for three times. The amount of heparin on the surface of PLGA NF scaffolds was measured by Toluidine Blue assay [22].

VEGF modification: 100 $ngmL^{-1}$ of VEGF ($VEGF_{165}$, PeproTech, UK) solution in 1% BSA was added to PLGA NF, NF-NH_2, and NF-Heparin scaffolds and incubated overnight at 4°C. All scaffolds were washed with PBS for three times after the reaction.

To quantify the amounts of immobilized VEGF on scaffolds, the concentration of remaining VEGF solution after immobilization reaction was measured by the ELISA kit following the recommendation of the manufacturer (Elabscience, China) [12].

To visualize the immobilized VEGF on scaffolds, immunofluorecence staining of the scaffolds was undertaken [23]. After immersed in 100 ng/mL VEGF solution at 4 °C overnight, NF, NF-NH_2, and NF-Heparin scaffolds were stained using rabbit anti-human VEGF primary antibody (1:200, Santa Cruz, USA) and Alex488-conjugated mouse anti-rabbit secondary antibody (1:200, Invitrogen, USA). Fluorescence microscope (Leica, Gemany) with fixed imaging parameters were used across all samples.

To test the sustained releasing of VEGF, PLGA NF, NF-NH_2, NF-VEGF scaffolds were incubated in PBS at 37 °C up to 31 days. At predetermined time points, 100 μL releasing VEGF solution was collected and analyzed by a modified ELISA assay (ELISA kit, PeproTech, USA) according to the manufacturer's instructions.

Characterization of surface wettability

Water contact angles were measured to determine the wettability of PLGA NF, NF-NH_2, and NF-VEGF scaffolds. Three samples of each group were measured by dropping 4 μL

dH_2O onto the surface and the droplet images were taken in 3 seconds by an Olympus camera. ImageJ software was used to analyze the images to obtain the contact angles of samples.

Effects of surface modification on the viability of cells

MSCs, isolated from Sprague-Dawley rats' bone marrow as described in our previous study [20], were cultured in α-MEM (Biosera, UK) supplemented with 10% FBS (Biosera, UK) and 1% Penicillin/streptomycin (A+A, Lonza, UK) under 37 °C and 5% CO_2. Ten thousand passage 2 MSCs were seeded onto each scaffold of PLGA NF, NF-NH_2, NF-Heparin and NF-VEGF. The viability of MSCs on the surface of each group at day 5 culture was determined by live and dead staining assay (Cellstain double staining kit, Sigma, USA). Confocal microscopy (Olympus, USA) with 490 nm and 535 nm excitation was used to observe the cell survival rate.

Proliferation study of HUVECs and MSCs co-culture

Human MSCs were isolated from human bone marrow mononuclear cells (Lonza, UK) by culturing in flasks coated with fibronectin (R&D System, UK) in low glucose DMEM (Biosera, UK) supplemented with 10% FBS and 1% A+A under 37 °C and 5% CO_2. Passage 3-5 of human MSCs were used in this study.

In the study of MSCs co-cultured with endothelial cells, MSCs derived from rats and human bone marrow (rMSCs and hMSCs) were used. HUVECs were purchased from GIBCO (Life Technologies, USA) and cultured in M200 media with low serum growth supplementary (LSGS, GIBCO, USA). HUVECs and r/hMSCs were co-cultured (rMIX and hMIX) on the surfaces of PLGA NF and NF-VEGF at a ratio of 1:9 with the total loading density of 2×10^4 cm^{-2} in a mixed medium by 1:1 α-MEM/M200 (MIX media). As control groups, r/hMSCs were mono-cultured in the same condition respectively.

Cell proliferation was tested by Cell Counting Kit-8 (CCK-8, Dojindo, Japan) as described in our previous study [20]. Briefly, at 1, 4, and 7 days after cell seeding, 220 μL of CCK-8 solutions at a dilution of 1:10 with MIX media were added to each sample and cultured at 37 °C with 5% CO_2. Two hours later, 100 μL of media were transferred to 96-well plate to measure absorption value at a wavelength of 450 nm using a microplate reader (Symergy HT, BioTek, USA).

Differentiation study of co-cultured HUVECs and MSCs

After co-cultured in MIX media for 1 week, rMSCs, rMIX, hMSCs, and hMIX on scaffolds of PLGA NF and NF-VEGF were changed into osteogenic condition, in which contained 50% M200 (supplemented with LSGS) and 50% osteogenic media (low glucose DMEM supplemented with 10% FBS, 1% A+A, 10 mmol/L glycerol phosphate, 10 $nmolL^{-1}$

dexamethasone, 50 μmolL^{-1} L-ascorbic acid, 300 mgL^{-1} L-glutamine and 10 nmolL^{-1} 1α, 25-dihydroxyvitamin D3 (Sigma-Aldrich, USA)). The media were changed every three days.

Alizarin Red staining: In order to stain the calcium mineralization on NF and NF-VEGF scaffolds, samples with rMSCs, rMIX, hMSCs, and hMIX were fixed with 70% ethanol for 1 hour at room temperature after cultured for 28 days. After washed once with tape water, samples were immersed into 40 mM Alizarin red S (ARS, Sigma, USA) for 20 min and then washed five times with tape water. All samples were observed under bright field microscopy. To quantify the calcium mineralization, ImageJ was used to analyze the percentage of stained area.

SEM-EDX analysis: The calcuim element distribution within the cells was analyzed using SEM in combination with energy dispersive X-ray analysis (SEM-EDX) (TM-3000, Hitachi, Japan). The elemental distribution of Calcium was mapped and analyzed.

ALP staining: Alkaline phosphatase (ALP) staining was conducted using an ALP kit (Millipore, UK). All samples were fixed with 4% paraformaldehyde for 2 minutes and stained following the kit instructions. The staining samples were observed under microscope. ImageJ was used to quantify the percentage of ALP stained area.

CD31 immunofluorescence staining: The effect of NF-VEGF scaffolds on CD31, the specific marker of HUVECs, expression, co-cultured HUVECs/r/hMSCs were investigated by immunofluorescence staining at day 21 culture. All samples were rinsed twice with PBS and fixed in 4% of PFA for 30 minutes at room temperature. The fixed samples were immersed in 1% bovine serum albumin (BSA)/PBS blocking buffer for 1 hour at 37 °C, and then were incubated with rabbit anti-rat CD31 primary antibody (1:200, Santa Cruz, UK) overnight at 4 °C. Then the samples were incubated in anti-rabbit secondary antibody TRITC (1:200, Santa Cruz, UK) for 2 hours at 37 °C. The samples were counterstained with DAPI (Abcam, USA) and visualized with a confocal microscopy (Olympus, USA). To quantify the angiogenesis, ImageJ was used to analyze the percentage of CD31 stained area.

Statistical analysis

All quantitative results are expressed as mean ± standard deviation. N = 3 were for treated groups. Statistical analysis was carried out using one-way ANOVA and t-test for each two group comparisons to determine significance. A value of $P<0.05$ was considered to be statistically significant.

Results

Biomimetically conjugation of VEGF on PLGA NF scaffolds

PLGA electrospinning fibers: Electrospinning technique produced PLGA nonwoven nanofibers with 588.9 ± 110.3 nm in diameter. SEM image in Figure 2A shows the morphology of PLGA NF and the inset shows the diameter distribution of nanofibers. The PLGA NF scaffolds exhibited a structure similar to extracellular matrix with pore structure and fibers with diameter ranged from 350 nm to 960 nm.

Heparin modification: PLGA NF modification was performed according to the procedure shown in Figure 1. Amine groups were grafted to NF surface by ammonia plasma treatment, after which heparin was conjugated using EDC/Sulfo-NHS which can activate carboxylic acid groups of heparin. According to the toluidine blue assay results (Figure 2B), 1.73 ± 0.06 μgcm^{-2} heparin was conjugated to NF-NH_2 scaffolds, indicating that the heparin modification of PLGA nanofibrous scaffolds was successful.

VEGF immobilization and releasing: Biomimetically conjugation of VEGF was accomplished through affinity binding with heparin. Figure 2C shows the release kinetics of VEGF from the electrospun PLGA NF with or without heparin conjugation. When VEGF was reacted with NF scaffolds without any treatment, the resulted scaffolds showed a low and abrupt initial burst release over the first 3 days of study. Almost no more additional release of VEGF was seen over the remaining experimental days. When VEGF was reacted with NF-NH_2 scaffolds without of heparin conjugated, the resulted scaffolds showed released VEGF to

5 days, after which no more releasing was detected. In contrast, a sustained release of VEGF in NF-heparin scaffolds was observed up to 31 days. The immunofluorecence staining and ELISA results of remaining reaction solutions indicated that VEGF grafting was siginificantly more efficient on NF-Heparin surface than the NF and NF-NH_2 surface (Figure 2E-H).

Contact angle: The surfaces wettability of modified PLGA substrates were evaluated by measuring contact angle according to our previous study [24]. The water contact angle on the ammonia plasma treated PLGA NF was dramatically decreased from 84.08 ± 1.30 to 39.23 ± 1.09 (Figure 2D). In addition, VEGF modified PLGA NF displayed the lowest contact angle (21.94 ± 3.81). The water droplet images on NF, NF-NH_2, and NF-VEGF scaffolds surfaces are presented in Figure 2D.

Biocompatibility of NF modification: Figure 3 shows the cell viability on the surfaces of NF, NF-NH_2, NF-Heparin, and NF-VEGF after seeded 5 days. It can be seen that most of MSCs attaching to PLGA NF were alive (green staining), while a few of them showed round shape and red fluorescence (dead cells) (Figure 3A1-A4). After ammonia plasma treatment and heparin conjugation, cell biocompatibility of PLGA NF was improved and the number of round and dead cells decreased (Figure 3B1-B4, C1-C4). On the surface of NF-VEGF, the highest number of live and well spread cells was observed.

Species dependent response on proliferation and osteogenesis

Proliferation of r/hMSCs: Figure 4A, B, and C showed the morphology of rMSCs, hMSCs, and HUVECs at day 3 of passage 2. Figure 4D and E showed the proliferation of rMSCs, rMIX, hMSCs, and hMIX after seeded on the surfaces of NF and NF-VEGF for 1, 3 (4), and 7 days. From Figure 4D, it can be found that VEGF modification can promote cell proliferation both in rMSCs and rMIX groups. However, when cultured on neat NF scaffolds, rMSCs grew much slower than that on VEGF modified NF, neither mono-cultured nor co-cultured with HUVECs. Figure 4E shows that both hMIX and hMSCs proliferated along with cultured time, while hMIX growth was faster than hMSCs on both NF and NF-VEGF surfaces. There was no difference of cell proliferation between each two types of surface when seeded with hMSCs or hMIX.

Osteogenesis of r/hMSCs: The osteogenesis capacity of MSCs derived from rats or human marrow seeded on PLGA NF and NF-VEGF scaffolds were evaluated by ALP at day 7 and calcium deposit staining with Alizarin Red S and SEM-EDX after 4 weeks of culture. In Figure 5, calcium deposition staining (red area) can be found on both types of surfaces (NF and NF-VEGF) seeding with rMSCs or rMIX under the osteogenic media (Figure 5A-D). Co-cultured with HUVECs, rMSCs showed higher level of calcium deposition on both NF and NF-VEGF surfaces (Figure 5C-D). Furthermore, it can be found that in compared with VEGF modified surface, rat MSC mono-culture had higher calcium deposition on NF surface (Figure

5A and B). The area of ARS staining regions was quantified as shown in Figure 5E. The co-cultured samples showed much higher level of calcium deposition compared with rMSCs mono-culture ($P<0.01$). The calcium element distribution results on NF and NF-VEGF surfaces detected by SEM-EDX analysis further confirmed the osteogenic differentiation of rMIX (Figure S1).

Figure 6 shows ARS staining on PLGA NF and NF-VEGF surfaces when seeding human MSCs for both mono- and co-culture (hMSCs and hMIX) under osteogenic media (Figure 6A-D). It can be found that when cultured on NF, both hMSCs and hMIX showed higher osteogenesis level in comparison of that on NF-VEGF surface. However, co-cultured with HUVECs didn't enhanced the osteogenesis level of hMSCs no matter what type of surface is. The calcium deposition was quantified by analysis of ARS staining images (Figure 6E). It was revealed that the effect of VEGF on osteogenesis of hMSCs and hMIX were not significantly different and co-culture also had no significant effects on hMSCs' osteogenic differentiation ($P>0.05$).

ALP expression showed strong species and surface chemistry dependent pattern (Figure S2). In general, no VEGF treated surface exhibited higher ALP expression for both rat and human MSC samples than NF-VEGF surface and co-culture of rat MSC with HUVECs demonstrated the highest APL expression.

Enhancement of angiogenesis by the immobilized VEGF and co-culture

VEGF effects on angiogenesis: The angiogenesis capacity of MSCs derived from rats or human bone marrow seeded on PLGA NF and NF-VEGF scaffolds were evaluated by CD31 immunofluorescence staining after 3 weeks of culture. CD31 expression of cells on PLGA NF and NF-VEGF surfaces were recorded by confocal microscopy. The fluorescence images of the CD31 expression were quantified as shown in Figure **7**A1-D2. To eliminate the effects of cell number, the expression of CD31 was normalized by nuclei stained by DAPI. As shown in Figure 7A1 and B1, C1 and D1, VEGF immobilized on NF enhanced the expression of CD31 in rat MSCs mono- and co-culture (rMSCs and rMIX) in comparison to on PLGA NF surfaces. Interestingly, rMIX cultured on NF-VEGF scaffolds formed cell aggregates, which never showed when rMSCs seeded alone. Figure 7E showed the quantification of CD31 staining area normalized by nucleus according to the fluorescence images in Figure 7A-D.

Similarly CD31 expression of hMSCs and hMIX culture on the surfaces of NF-VEGF was significantly enhanced in comparison to on PLGA NF surface as shown in Figure 8.

Co-culture enhanced angiogenesis: It can be seen from Figure 7 that rMSCs and HUVECs co-cultured groups had higher CD31 expression than rMSCs mono-cultured groups on both PLGA NF and NF-VEGF surfaces. From Figure 7E we can found that rMIX cultured on NF-

VEGF group had the highest CD31 expression than other groups, which indicated the synergistic effects of co-culture and VEGF on the angiogenesis of rMSCs. Comparing the CD31 staining area of rMSCs on NF-VEGF and rMIX on NF, we noticed that the two groups had similar CD31 expression level (P>0.05), indicating the analogous effects of VEGF and HUVECs on the angiogenic differentiation of rMSCs.

In Figure 8E, it showed that hMIX seeded on PLGA NF surface (Figure 8C) had higher CD31 expression than that hMSCs on NF surface (Figure 8A). However, comparing hMIX on NF-VEGF (Figure 8D) with hMIX on NF (Figure 8C) and hMSCs on NF-VEGF (Figure 8B), we noticed that the synergistic effects of co-culture and VEGF on the angiogenesis of hMSCs was not as obvious as rMSCs.

Discussion

One important role of scaffolds in tissue engineering is to serve as a vehicle for delivery of growth factors [25]. VEGF, one of the most important growth factors in angiogenesis, not only has effects on vascular invasion, but also can promote bone regeneration [7]. Therefore, various techniques have been employed to immobilize VEGF to bioactive and biomimetic polymer scaffolds, such as physical encapsulation, covalent binding, and affinity binding. Among these methods, affinity binding can mimic interactions between growth factors and

natural extracellular matrix and avoid the rapid degradation, which facilitated sustained releasing of growth factors [4]. Thus, in this study, VEGF was immobilized to PLGA NF scaffolds through heparin which has high affinity binding towards VEGF and can preserve the biological activity of VEGF [26]. Given the deficiency of amine groups reacting with heparin, PLGA NF were treated with ammonia plasma treatment to obtain NF-NH_2 scaffolds and then heparin molecules were covalently attached to NF-NH_2 surface via EDC/Sulfo-NHS. The contact angle changes, Toluidine Blue assay results, and the in vitro VEGF release kinetics all indicated that amine group, heparin, and VEGF have incorporated successfully to the surface of PLGA NF covalently and biologically. The release kinetics also showed that we accomplished sustained releasing of VEGF through affinity binding to heparin.

Live and dead staining results indicated the improved biocompatibility of NF after modified by plasma treatment, heparin and VEGF grafting. It has been demonstrated that ammonia plasma treatment can introduce amine groups to surface of polymer scaffolds and improve their cell compatibility [24]. While the anti-proliferation effect of heparin on vascular smooth muscle cells (SMCs) has been reported in previous research, which was in conflict with our results that heparin modified surface had better cell viability compared with neat NF surface. We speculated that this contradiction might come from the heparin supplementary methods in our study, in which rMSCs and conjugated heparin were used instead of SMCs and free heparin in other study [14].

It has been previously demonstrated that hMSCs co-cultured with HUVECs can support cell proliferation because of the cross talk between hMSCs and HUVECs [27]. Related findings were reported by Ma and colleagues who found that cell proliferation increased when HUVECs co-cultured with both human bone marrow derived MSCs and human adipose tissue derived MSCs [18]. Our study was consistent to that study and showed that HUVECs can enhance proliferation of hMSCs on both NF and NF-VEGF surfaces, while VEGF can promote the attachment and proliferation of rMSCs and rMIX. Both rMSCs and rMIX on NF showed lower attachment level compared with that on modified NF surfaces, which was in compliance with the live and dead staining results.

Co-culture of vascular endothelial cells and stem cells is one of the promising strategies to enhance vascularization in bone tissue engineering [28]. HUVECs and bone marrow derived MSCs were the most commonly used cell types [29]. In this study, we co-cultured HUVECs with MSCs from different species to evaluate their osteogenic and angiogenic differentiation efficiency on surface modified NF scaffolds. The differentiation results showed that angiogenesis was enhanced in both co-culture groups, rMIX and hMIX, which can be explained by the angiogenic differentiation of MSCs through the cross-talk between MSCs and HUVECs. Previous researchers investigated the in vivo and in vitro angiogenic capacity of MSCs-HUVECs and found that co-culture can enhance vascularization [30]. We noticed that

the CD31 expression of hMIX was much higher than that of rMIX on the scaffold surfaces, indicating that MSCs from different species could have diverse reactions when co-cultured with HUVECs. This speculation was confirmed by the supplementary evidence from osteogenic results, from which we found that rMIX had higher level of osteogenesis compared with rMSCs monoculture while there was no difference between hMSCs and hMIX. Song and colleagues found that endothelial progenitor cells (EPCs) and bone marrow stem cells (BMSCs) co-cultured together can promote angiogenesis but retard terminal differentiation of osteoblasts in bone regeneration by up-regulating Id1 [31]. However, most HUVEC-hMSC co-cultured experiments supported that co-culture can enhance osteogenesis than monoculture [17]. The mechanism needs further investigation.

Another interesting result conflicted with previous research in this study was that VEGF modified NF scaffolds cannot promote osteogenic differentiation of MSCs whether from rat bone marrow or from human bone marrow. Villars and colleagues noticed that early osteoblastic marker (ALP) levels increased when human bone marrow stromal cells were co-cultured with HUVEC in direct contact. However, unlike previous studies, they also did not find that VEGF increased these processes [32]. Given the high expression of CD31 in NF-VEGF groups, we speculated that this phenomenon can be explained by the competition reaction of MSCs to the osteogenic and angiogenic mixture media. On NF-VEGF surface, VEGF triggered the angiogenic signal pathways inside MSCs and angiogenic media induced

following angiogenesis procedure. There is an essential balance between angiogenic and osteogenic growth factors during bone healing and excessive concentration of VEGF may favorite endothelial cell differentiation over osteogenesis [4].

Conclusion

We successfully conjugated VEGF to PLGA nanofiber scaffold surface enabling bioactive VEGF releasing for 30 days. The angiogenic differentiation capacity of MSCs from both rat and human species have been enhanced significantly when culturing on the NF-VEGF scaffolds. The further enhancement, i.e. synergetic effect has been achieved when co-culturing the MSCs with HUVECs on the NF-VEGF scaffolds. The proliferation and osteogenic differentiation level of MSCs when culturing with HUVECs on NF-VEGF scaffolds showed a species dependent response. Specially, the osteogenic differentiation of rMSCs was greatly enhanced by co-culturing with HUVECs and on NF-VEGF scaffolds, whilst hMSCs co-culturing with HUVECs or culturing on NF-VEGF scaffolds including mono-culture inhibited the osteogenesis of hMSCs. Thus, this study demonstrates that VEGF immobilization and HUVECs co-culturing are good strategies for vascularization in bone tissue engineering. However, the species dependent property of MSCs should also be considered when the application was different.

Acknowledgements

This work was supported by EC FP7 Marie Curie International Incoming Fellowship; Jiangsu Key Laboratory of New Drug Research and Clinical Pharmacy, Xuzhou Medical College [grant number KF-XY201507]; Natural science foundation for colleges and universities in Jiangsu Province [grant number 16KJB310018]; Science and technology project of Xuzhou City [grant number KC16SY156].

References

[1] Camilo CC, Silveira CAE, Faeda RS, de Almeida Rollo JMD, Purquerio BM,Fortulan CA. Bone response to porous alumina implants coated with bioactive materials, observed using different characterization techniques. Journal of applied biomaterials & functional materials 2017;15:e223.

[2] Jin K, Li B, Lou L, Xu Y, Ye X, Yao K, Ye J,Gao C. In vivo vascularization of MSC-loaded porous hydroxyapatite constructs coated with VEGF-functionalized collagen/heparin multilayers. Scientific reports 2016;6:19871.

[3] Rouwkema J, Khademhosseini A. Vascularization and Angiogenesis in Tissue Engineering: Beyond Creating Static Networks. Trends in biotechnology 2016;34:733-45.

[4] Almubarak S, Nethercott H, Freeberg M, Beaudon C, Jha A, Jackson W, Marcucio R, Miclau T, Healy K,Bahney C. Tissue engineering strategies for promoting vascularized bone regeneration. Bone 2016;83:197-209.

[5] Acevedo LM, Barillas S, Weis SM, Gothert JR,Cheresh DA. Semaphorin 3A suppresses VEGF-mediated angiogenesis yet acts as a vascular permeability factor. Blood 2008;111:2674-80.

[6] Palmer BF,Clegg DJ. Oxygen sensing and metabolic homeostasis. Molecular and cellular endocrinology 2014;397:51-8.

[7] Hoeben A, Landuyt B, Highley MS, Wildiers H, Van Oosterom AT,De Bruijn EA. Vascular endothelial growth factor and angiogenesis. Pharmacological reviews 2004;56:549-80.

[8] Barabaschi GD, Manoharan V, Li Q,Bertassoni LE. Engineering Pre-vascularized Scaffolds for Bone Regeneration. Advances in experimental medicine and biology 2015;881:79-94.

[9] Saran U, Gemini Piperni S,Chatterjee S. Role of angiogenesis in bone repair. Archives of biochemistry and biophysics 2014;561:109-17.

[10] Zhang WJ, Wang XL, Wang SY, Zhao J, Xu LY, Zhu C, Zeng DL, Chen J, Zhang ZY, Kaplan DL,Jiang XQ. The use of injectable sonication-induced silk hydrogel for VEGF(165) and BMP-2 delivery for elevation of the maxillary sinus floor. Biomaterials 2011;32:9415-24.

[11] Kanczler JM, Ginty PJ, Barry JJ, Clarke NM, Howdle SM, Shakesheff KM,Oreffo RO. The effect of mesenchymal populations and vascular endothelial growth factor delivered from biodegradable polymer scaffolds on bone formation. Biomaterials 2008;29:1892-900.

[12] Shin YM, Lee YB, Kim SJ, Kang JK, Park JC, Jang W,Shin H. Mussel-inspired immobilization of vascular endothelial growth factor (VEGF) for enhanced endothelialization of vascular grafts. Biomacromolecules 2012;13:2020-8.

[13] Teran M,Nugent MA. Synergistic Binding of Vascular Endothelial Growth Factor-A and Its Receptors to Heparin Selectively Modulates Complex Affinity. The Journal of biological chemistry 2015;290:16451-62.
[14] Lee J, Yoo JJ, Atala A,Lee SJ. The effect of controlled release of PDGF-BB from heparin-conjugated electrospun PCL/gelatin scaffolds on cellular bioactivity and infiltration. Biomaterials 2012;33:6709-20.
[15] Patel S, Kurpinski K, Quigley R, Gao H, Hsiao BS, Poo MM,Li S. Bioactive nanofibers: synergistic effects of nanotopography and chemical signaling on cell guidance. Nano letters 2007;7:2122-8.
[16] Chamberlain G, Fox J, Ashton B,Middleton J. Concise review: mesenchymal stem cells: their phenotype, differentiation capacity, immunological features, and potential for homing. Stem Cells 2007;25:2739-49.
[17] Bidarra SJ, Barrias CC, Barbosa MA, Soares R, Amedee J,Granja PL. Phenotypic and proliferative modulation of human mesenchymal stem cells via crosstalk with endothelial cells. Stem cell research 2011;7:186-97.
[18] Ma J, Yang F, Both SK, Prins HJ, Helder MN, Pan J, Cui FZ, Jansen JA,van den Beucken JJ. In vitro and in vivo angiogenic capacity of BM-MSCs/HUVECs and AT-MSCs/HUVECs cocultures. Biofabrication 2014;6:015005.
[19] Chang NJ, Lin CC, Li CF, Wang DA, Issariyaku N,Yeh ML. The combined effects of continuous passive motion treatment and acellular PLGA implants on osteochondral regeneration in the rabbit. Biomaterials 2012;33:3153-63.
[20] Lu LX, Zhang XF, Wang YY, Ortiz L, Mao X, Jiang ZL, Xiao ZD,Huang NP. Effects of hydroxyapatite-containing composite nanofibers on osteogenesis of mesenchymal stem cells in vitro and bone regeneration in vivo. ACS applied materials & interfaces 2013;5:319-30.
[21] Wang Z, Sun B, Zhang M, Ou L, Che Y, Zhang J,Kong D. Functionalization of electrospun poly(ε-caprolactone) scaffold with heparin and vascular endothelial growth factors for potential application as vascular grafts. Journal of Bioactive and Compatible Polymers 2012;28:154-66.
[22] Janairo RR, Henry JJ, Lee BL, Hashi CK, Derugin N, Lee R,Li S. Heparin-modified small-diameter nanofibrous vascular grafts. IEEE transactions on nanobioscience 2012;11:22-7.
[23] Su ZQ, Li JF, Ouyang ZF, Arras MML, Wei G,Jandt KD. Biomimetic 3D hydroxyapatite architectures with interconnected pores based on electrospun biaxially orientated PCL nanofibers. Rsc Adv 2014;4:14833-9.
[24] Wang YY, Lu LX, Shi JC, Wang HF, Xiao ZD,Huang NP. Introducing RGD peptides on PHBV films through PEG-containing cross-linkers to improve the biocompatibility. Biomacromolecules 2011;12:551-9.
[25] Amini AR, Laurencin CT,Nukavarapu SP. Bone tissue engineering: recent advances and challenges. Critical reviews in biomedical engineering 2012;40:363-408.

[26] Yoon JJ, Chung HJ, Lee HJ,Park TG. Heparin-immobilized biodegradable scaffolds for local and sustained release of angiogenic growth factor. Journal of biomedical materials research Part A 2006;79:934-42.
[27] Gershovich JG, Dahlin RL, Kasper FK,Mikos AG. Enhanced osteogenesis in cocultures with human mesenchymal stem cells and endothelial cells on polymeric microfiber scaffolds. Tissue engineering Part A 2013;19:2565-76.
[28] Paschos NK, Brown WE, Eswaramoorthy R, Hu JC,Athanasiou KA. Advances in tissue engineering through stem cell-based co-culture. Journal of tissue engineering and regenerative medicine 2015;9:488-503.
[29] Kang Y, Kim S, Fahrenholtz M, Khademhosseini A,Yang Y. Osteogenic and angiogenic potentials of monocultured and co-cultured human-bone-marrow-derived mesenchymal stem cells and human-umbilical-vein endothelial cells on three-dimensional porous beta-tricalcium phosphate scaffold. Acta biomaterialia 2013;9:4906-15.
[30] Brennan M, Davaine JM,Layrolle P. Pre-vascularization of bone tissue-engineered constructs. Stem cell research & therapy 2013;4:96.
[31] Song X, Liu S, Qu X, Hu Y, Zhang X, Wang T,Wei F. BMP2 and VEGF promote angiogenesis but retard terminal differentiation of osteoblasts in bone regeneration by up-regulating Id1. Acta biochimica et biophysica Sinica 2011;43:796-804.
[32] Villars F, Bordenave L, Bareille R,Amedee J. Effect of human endothelial cells on human bone marrow stromal cell phenotype: role of VEGF? Journal of cellular biochemistry 2000;79:672-85.

Figure Captions

Figure 1 Schematic diagram of PLGA nanofibers modification process. Ammonia plasma treatment was done to introduce amine group to PLGA NF, and then heparin was grafted through crosslinker of EDC/NHS, finally, VEGF was covalently banded to NF-Heparin surface.

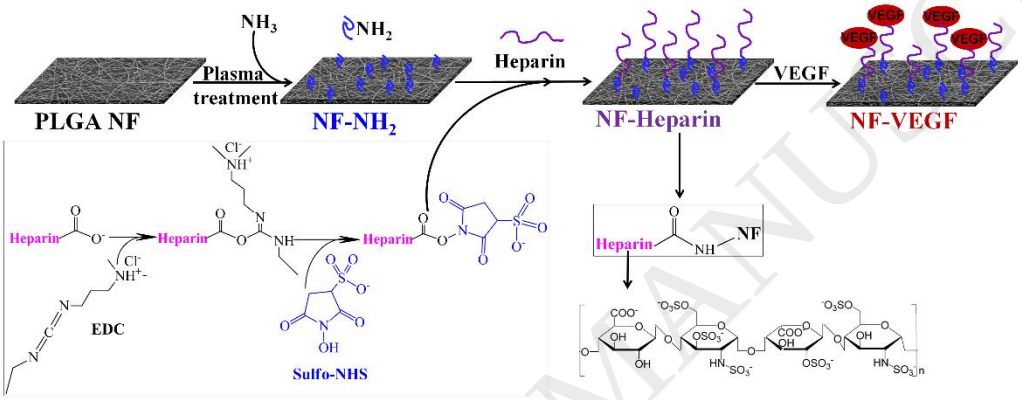

Figure 2 A: SEM image of PLGA NF, inserted: distribution of fibers diameters (588.89 ± 110.28 nm); B: The amount of heparin conjugation was quantified by Toluidine Blue assay; C: VEGF releasing from different surface (NF, NF-NH_2, and NF-Heparin) quantified by ELISA assay; D: Surface wettability tested by water contact angle, inserted images: water droplet on films. E-G: Immunofluorescence images of NF (E), NF-NH_2 (F), and NF-Heparin (G) to show the VEGF modification. H: ELISA result to show the quantified VEGF modification.

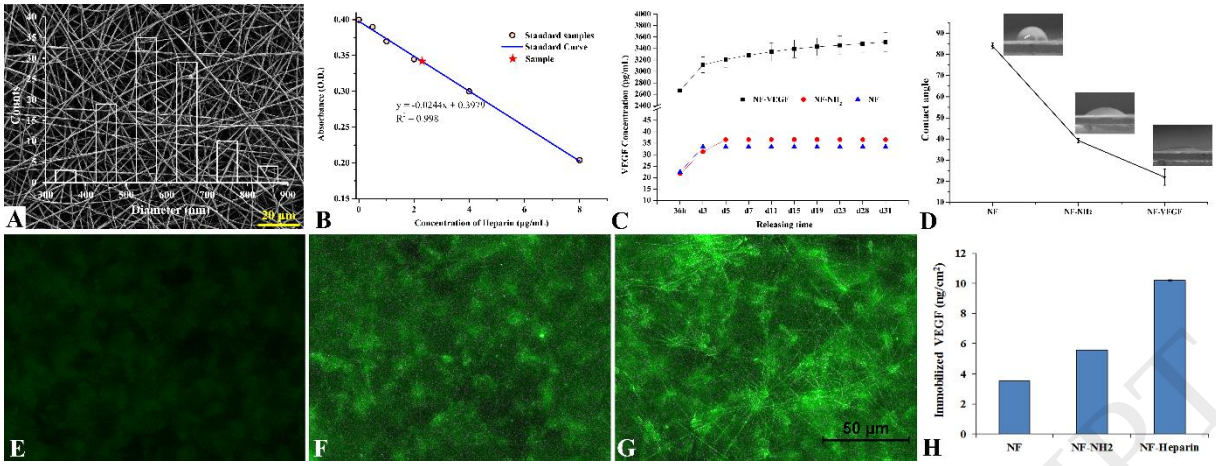

Figure 3. Live & Dead staining of rMSCs cultured on NF (A1-A4), NF-NH_2 (B1-B4), NF-Heparin (C1-C4), and NF-VEGF (D1-D4) at day 5. A1-D1: bright field images; A2-D2: live cells (green); A3-D3: dead cells (red); A4-D4: merged. Scale bar: 200 μm

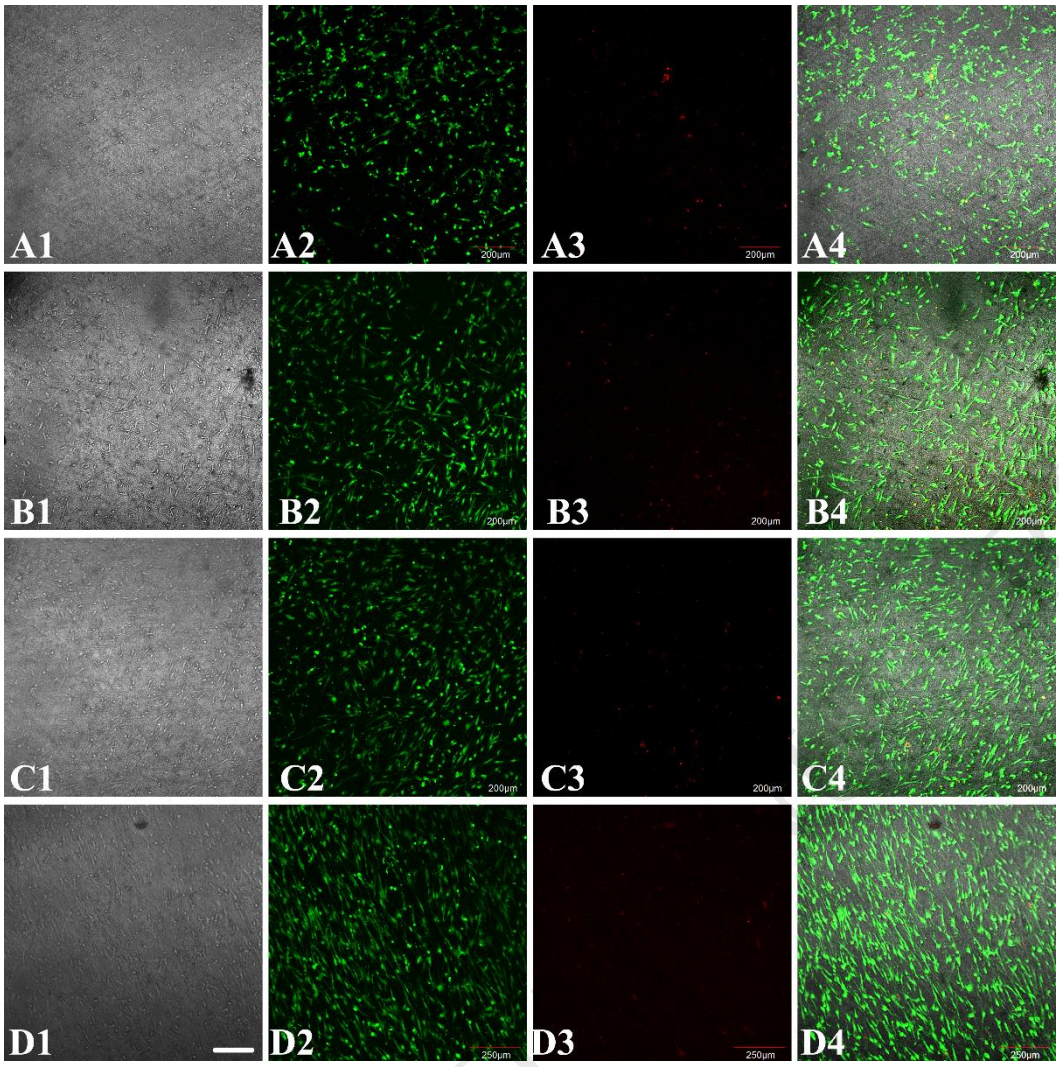

Figure 4. A-C: Cell morphology observed by microscopy at day 3 of passage 2 (A: rMSCs, B: hMSCs, C: HUVECs); D-E: r/hMSCs proliferation with and without HUVECs seeded on PLGA NF and NF-VEGF surfaces (D: CCK-8 results of rMSCs/rMIX, E: CCK-8 results of hMSCs/hMIX).

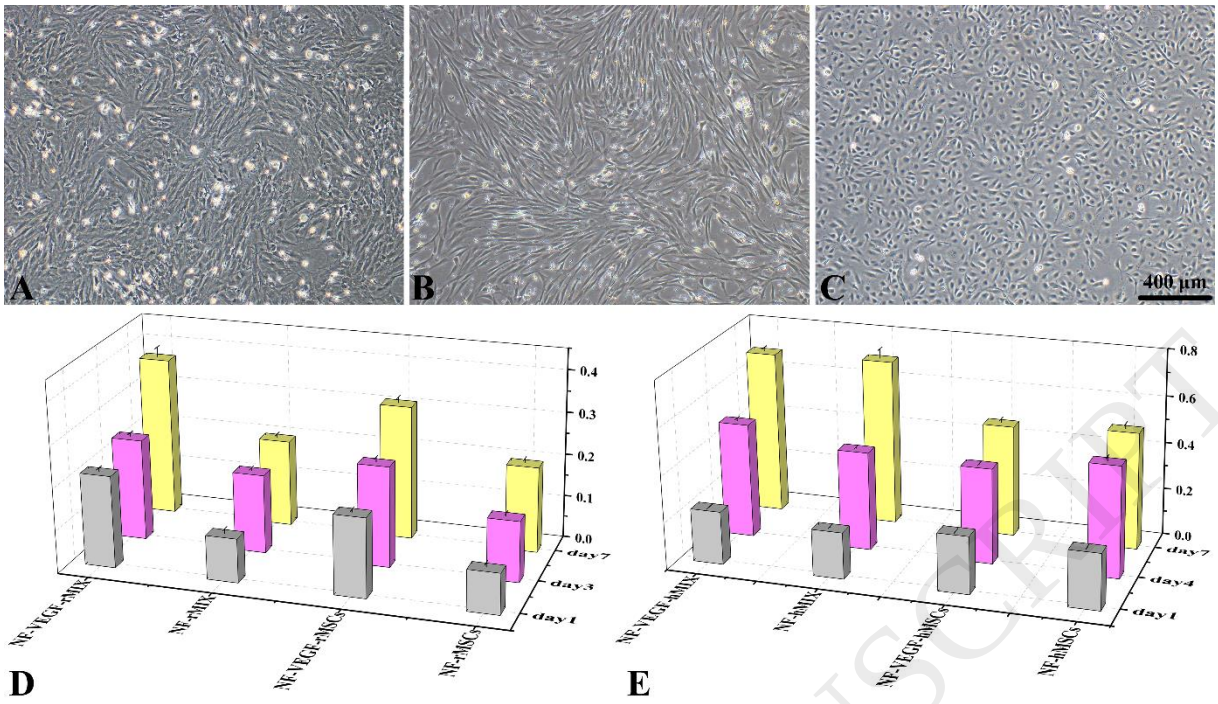

Figure 5. Alizarin Red S staining results observed by microscopy at day 28 to show the osteogenic of rMSCs cultured on PLGA NF (A), NF-VEGF (B), and rMIX cultured on NF (C) and NF-VEGF (D). A1-D1: Black-white images of A-D processed using Image J software. E: The graph shows the area of ARS positive regions for the different study groups. (#: $P>0.05$, *$P<0.05$). Scale bar: 400 μm

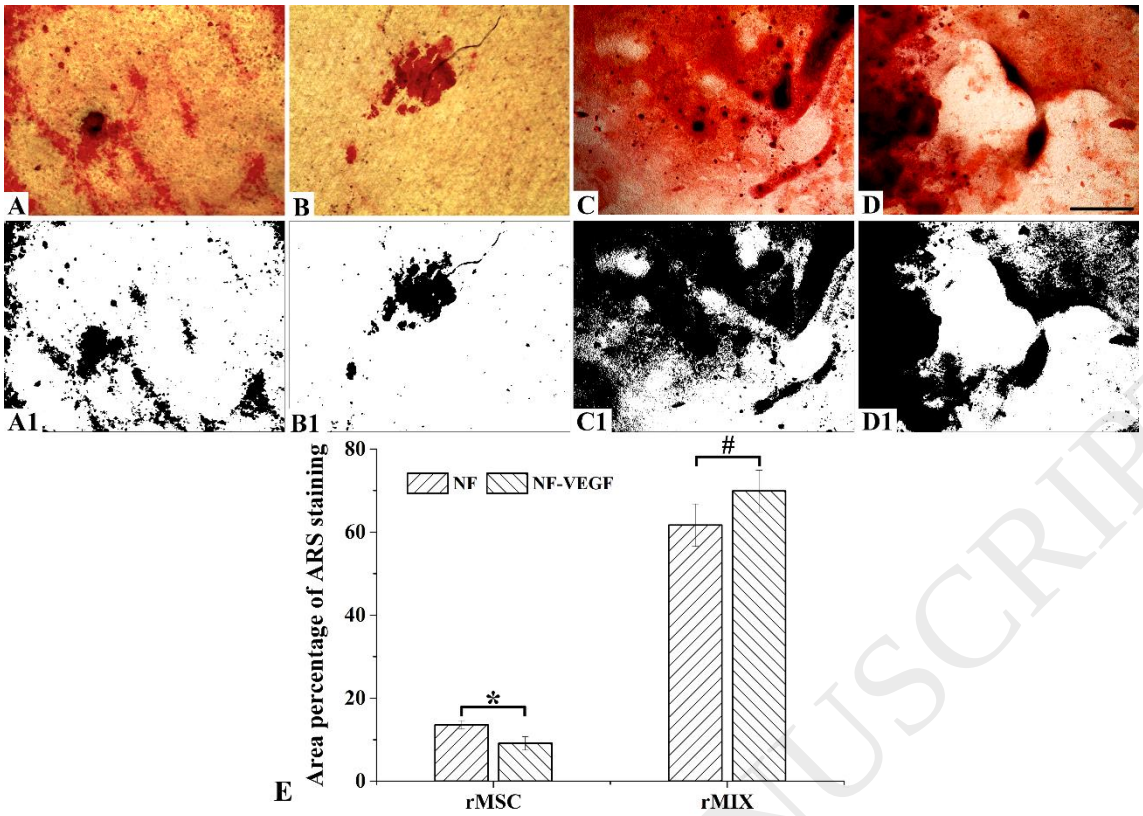

Figure 6. Alizarin Red S staining results observed by microscopy at day 28 to show the osteogenic of hMSCs cultured on PLGA NF (A), NF-VEGF (B), and hMIX cultured on NF (C) and NF-VEGF (D). A1-D1: Black-white images of A-D processed using Image J software. E: The graph shows the area of ARS positive regions for the different study groups. (*P<0.05). Scale bar: 400 μm

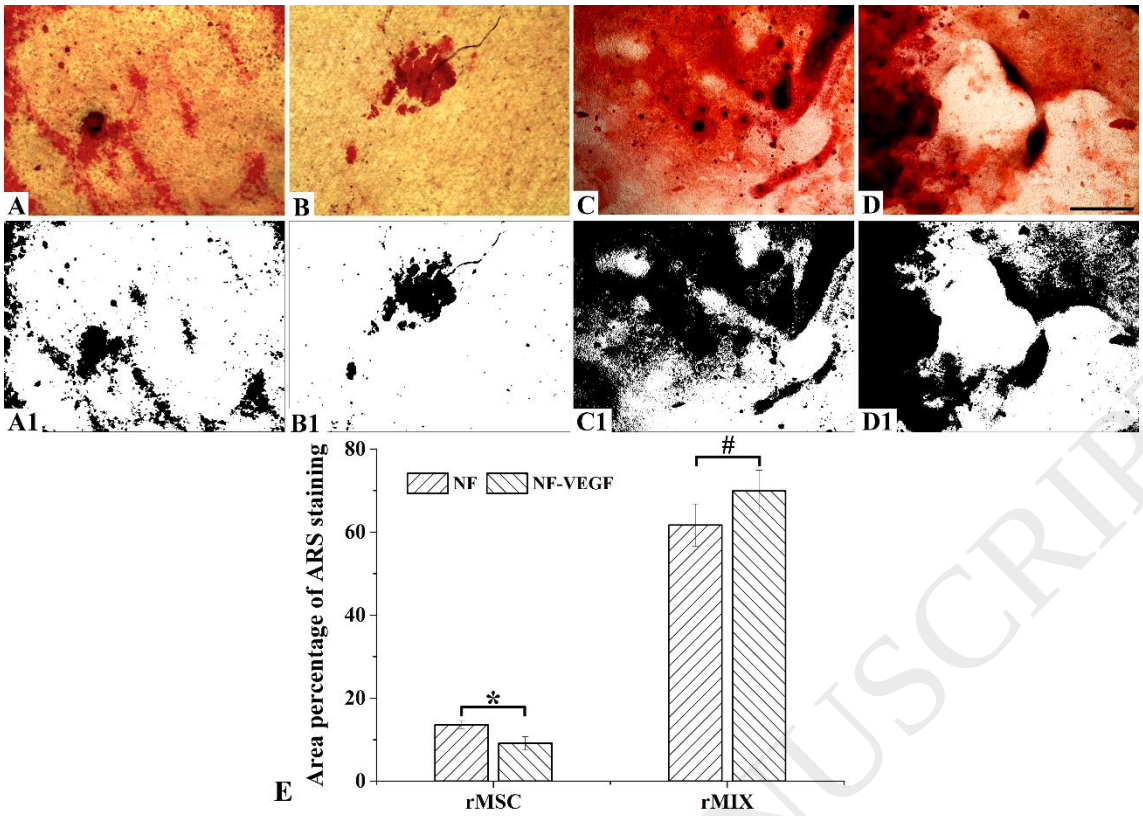

Figure 7. CD31 immunofluorescence staining of rMSCs and rMIX cultured on PLGA NF and NF-VEGF to show the angiogenic of cells. A1-A3: rMSCs on NF; B1-B3: rMSCs on NF-VEGF; C1-C3: rMIX on NF; D1-D3: rMIX on NF-VEGF. (Red: CD31; Blue: nucleus) E: The CD31 staining area normalized by nucleus. (**P*<0.05).

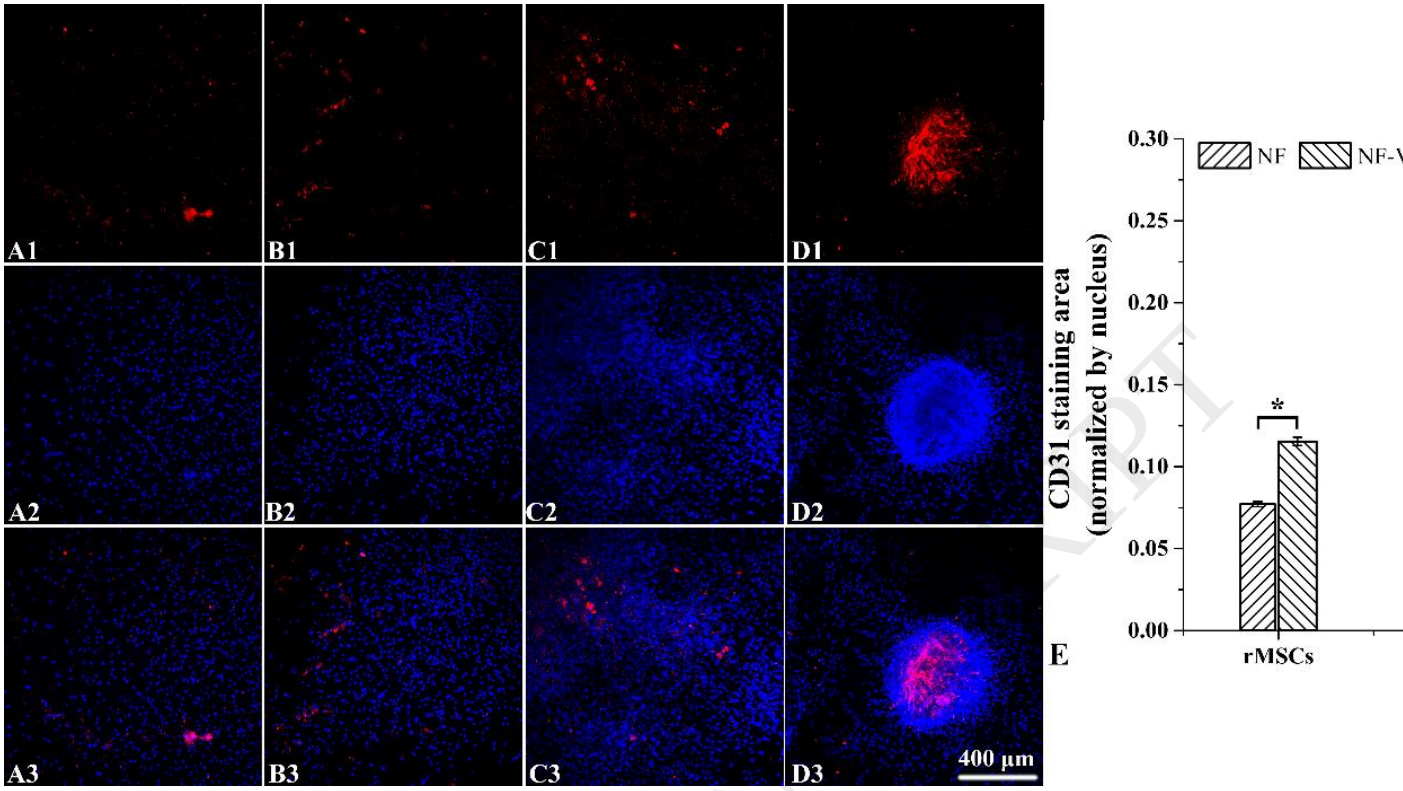

Figure 8 CD31 immunofluorescence staining of hMSCs and hMIX cultured on PLGA NF and NF-VEGF to show the angiogenic of cells. A1-A3: hMSCs on NF; B1-B3: hMSCs on NF-VEGF; C1-C3: hMIX on NF; D1-D3: hMIX on NF-VEGF. (Red: CD31; Blue: nucleus) E: The CD31 staining area normalized by nucleus. (#: $P>0.05$, *$P<0.05$).